physica status solidi

pss

www.pss-journals.com

reprint

WILEY-VCH

Phys. Status Solidi A **208**, No. 11, 2587–2590 (2011) / **DOI** 10.1002/pssa.201184263

physica status solidi a
www.pss-a.com
applications and materials science

Study of oxide precipitates in silicon using X-ray diffraction techniques

Ondřej Caha*[,1], Silvie Bernatová[1], Mojmír Meduňa[1], Milan Svoboda[2], and Jiří Buršík[2]

[1] Department of Condensed Matter Physics and CEITEC, Masaryk University, Kotlářská 2, 611 37 Brno, Czech Republic
[2] Institute of Physics of Materials, Academy of Sciences of the Czech Republic, Brno, Czech Republic

Received 28 November 2010, accepted 27 June 2011
Published online 7 October 2011

Keywords high-resolution X-ray diffraction, oxide precipitates, silicon

* Corresponding author: e-mail caha@physics.muni.cz, Phone: +420-549493388, Fax: +420-541211214

The results of a study of oxide precipitates in Czochralski (CZ) grown silicon using two X-ray diffraction methods are reported. The diffuse scattering around the Bragg diffraction maxima was measured on a series of samples after various two-stage annealing treatment. Combining the analysis of diffuse scattering with other experimental techniques we were able to determine mean precipitate size and deformation field around the precipitates. The obtained data show that the deformation field is proportional to the precipitate volume and independent on the annealing temperature or annealing time. The dynamical diffraction in Laue geometry was used to measure precipitate concentration. The results are compared to the selective etching concentration measurement.

1 Introduction Silicon wafers sliced from Czochralski (CZ) grown silicon single crystals involve certain amount of dissolved oxygen incorporated from quartz crucible during the crystal pulling. The thermal history of such a crystal gives rise to creation of series of point defects including the growth of oxygen precipitates. However the structural quality of semiconductor wafers and epitaxial layers is an important parameter substantially influencing their electric parameters and decrease the performance of fabricated integrated circuits. On the contrary the defects can also be beneficial, since they can getter out impurities, especially heavy metal atoms. Thus a reliable control of the defect nucleation and growth during the semiconductor technology is an important issue.

The X-ray diffuse scattering around reciprocal lattice point has been used to study precipitates in silicon and other defects like dislocation loops for a long time [1–3]. However, the defect size determined using X-ray diffuse scattering is usually much larger than the size of the SiO_2 precipitate itself. In this paper we study the defect size determined by X-ray diffuse scattering and compare that value to the precipitate size obtained by infrared (IR) absorption spectroscopy and selective etching. From that comparison we determine the deformation field around oxide precipitates in silicon and we obtain that the volume expansion of the precipitate is almost independent on the precipitate size. On the other hand the diffuse scattering gives us only limited information of absolute precipitate concentration. In order to determine the absolute concentration, we have also performed measurements of diffraction curves in Laue geometry which were simulated by dynamical diffraction theory based on Takagi equations.

2 Experiment The investigated samples were cut from low boron doped CZ grown silicon (111) wafer. The wafer came from the part of the ingot with the interstitial oxygen concentration of $7.3 \times 10^{17}\,\mathrm{cm}^{-3}$. In order to dissolve the nuclei of precipitates formed during ingot cooling process, the samples were first pre-annealed for 6 min at 1000 °C. The following temperature process consisted of 24 h nucleation annealing at 600 °C and subsequent precipitation annealing at various temperatures in the range from 800 to 950 °C up to 144 h. The series of samples was prepared varying the length and temperature of precipitation annealing. The precipitate nuclei were formed during the nucleation annealing stage at relatively high concentrations from 1 to $3 \times 10^{11}\,\mathrm{cm}^{-3}$. The lower precipitation temperature allows smaller nuclei to grow and therefore the process leads to higher precipitate concentration.

The high-resolution diffractometer with a conventional Cu X-ray tube was used for both types of X-ray diffraction

experiments. The beam optics consisted of a parabolic multilayer mirror and a Bartels-type Ge (220) monochromator. The reciprocal space maps (RSM) of X-ray scattered intensity were measured using a point detector with a channel-cut analyzer. The diffraction curves in Laue geometry were measured using two point detectors without any analyzer, one for diffracted beam and the other for the beam transmitted through the sample. In order to measure the Laue diffraction, we have cut and polished thin slices from the original thick wafers. The thickness of slices varied from 130 to 200 μm, which is two to three times larger than extinction length of the Cu Kα radiation in silicon.

The IR absorption spectroscopy was performed on a Fourier transform Bruker IFS Equinox spectrometer in a spectral range from 400 to 6000 cm^{-1} at room and liquid nitrogen temperatures in order to distinguish between the absorption peak of interstitial oxygen and SiO_x precipitates. The interstitial oxygen concentration was determined according to Ref. [4], using NewASTM calibration factor.

3 X-ray diffuse scattering Examples of measured RSMs around (111) diffraction point on two samples annealed at 850 °C are presented in Fig. 1. A crystal truncation rod (CTR) perpendicular to sample surface and an analyzer streak (AS) along the detector scan induced by the dynamical diffraction effect from sample and analyzer crystal are evident in these RSMs. The remaining diffusely scattered intensity originating from precipitates is symmetrically distributed with respect to the Q_z-axis. Longer annealing time leads to the higher diffuse scattered intensity.

More detailed analysis can be done studying cuts extracted from the RSMs. The cuts through the diffraction peak along Q_x-axis of the maps shown in Fig. 1 are plotted in Fig. 2. One can see two regions where scattered intensity depends on Q_x as $I \sim Q^{-1}$ and $I \sim Q^{-3}$. Such dependence is generally valid for volume defects in a distorted crystal lattice [5, 6]. Standard diffraction theory interprets the region further from the reciprocal lattice point, where intensity decays as $I \sim Q^{-3}$, as a Stokes–Wilson scattering on the

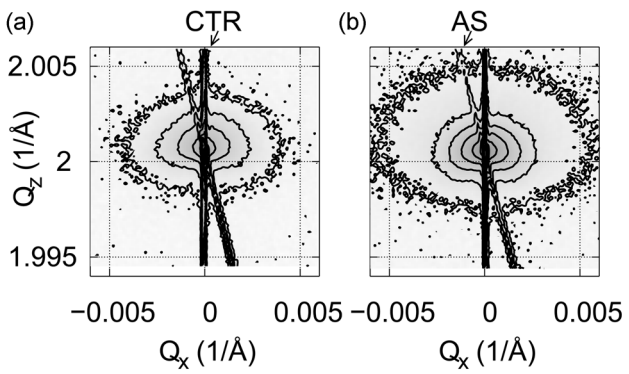

Figure 1 Reciprocal space maps around (111) reciprocal lattice point for samples annealed at 850 °C for 48 h (left panel) and 120 h (right panel). CTR and AS denote crystal truncation rod of the sample and analyzer streak, respectively.

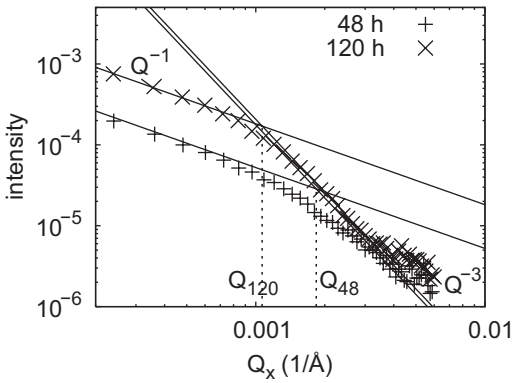

Figure 2 Cuts through the reciprocal space maps shown in Fig. 1. The region close to CTR is omitted from the plot.

amorphous defect core. The scattering near the reciprocal lattice point can be explained as a Huang scattering on the lattice deformed by a point defect. The displacement u outside spherical precipitate in the isotropic material is given by the formula:

$$u(r) = \frac{pV}{4\pi r^2}, \tag{1}$$

where V is precipitate volume, r distance from the defect center, and p is the mismatch of the unstrained and real precipitate volume. The size of the defect is usually determined from the reciprocal space position Q_t, where the intensity dependence transforms from $I \sim Q^{-1}$ dependence to $I \sim Q^{-3}$ (see Fig. 2). We have determined the transition point Q_t as the intersection of the lines fitted in the Huang and Stokes–Wilson regions as shown in Fig. 2.

However, the intensity dependence $I \sim Q^{-1}$ can be derived only if the deformation is small $hu \ll 1$ and the following exponential can be approximated by the first term in the Taylor expansion:

$$e^{-i\boldsymbol{h}\cdot\boldsymbol{u}(r)} - 1 \approx -i\boldsymbol{h}\cdot\boldsymbol{u}(\boldsymbol{r}), \tag{2}$$

where $\boldsymbol{h}$ is reciprocal lattice vector of the measured diffraction. In our previous work we have shown that the intensity distribution scattered on the strongly deformed region averaged over the various precipitate sizes leads to the intensity dependence Q^{-3}, which is same behavior as the Stokes–Wilson scattering on the non-diffracting precipitate core [7]. In such a case the whole region of the SiO_2 precipitate itself and the surrounding region of large deformation act as a non-diffracting parts of the crystal and we cannot determine the size of just the precipitate from the X-ray diffraction. However, we can determine radius of the strongly deformed region R_d using transition point position Q_t according to the formula $R_d = \pi/Q_t$.

The strongly deformed region is a part of crystal, where the higher order term in the Taylor expansion (2) cannot be neglected. The value of the neglected terms is proportional to the product $\boldsymbol{h}\cdot\boldsymbol{u}(\boldsymbol{r})$. Therefore the size of strongly deformed

region depends on the length of the diffraction vector $\boldsymbol{h}$. We have shown in our previous article [7] that the approximation (2) can be used outside region of radius R_d:

$$hu(r > R_d) \leq 0.1, \quad u(R_d) = \frac{0.1}{h}, \quad u(R_d) = 0.016d, \tag{3}$$

where $d = 2\pi/h$ is interplanar distance for certain diffraction. In the other words the term strong deformation means that the displacement is higher than about 1.6% of the interplanar distance of the corresponding diffraction. Combining the formulas (1) and (3) one can easily obtain:

$$R_d^2 = 10\frac{pVh}{4\pi}. \tag{4}$$

It is worthy to note, that the radius of the strongly deformed region R_d is proportional to the square-root of the diffraction vector $\boldsymbol{h}$. Such behavior was observed for our samples [7] and also earlier for the dislocation loops [8].

Combining the volume ratio of the oxide precipitates in the silicon matrix obtained from the IR absorption spectroscopy measurement and the precipitate concentration calculated from the selective etching measurement, we can determine the mean precipitate volume. The dependence of the square of the deformed region radius R_d^2 on the precipitate volume V should be linear according to the formula (4). The experimental behavior is plotted in Fig. 3. The points for the samples annealed at 800, 850 °C and also some points for samples annealed at 900 °C correspond very well to the line for mismatch value $p = 0.08$. This is an important results indicating that the precipitate mismatch is independent on precipitate size and precipitation temperature for temperatures below 900 °C. The points measured by the samples annealed at the temperature 950 °C give much larger radius of the deformed region than the samples annealed at lower temperatures. Analyzing the transmission electron microscopy (TEM) images (see, e.g., in Fig. 4), one can observe that the precipitation annealing at temperatures

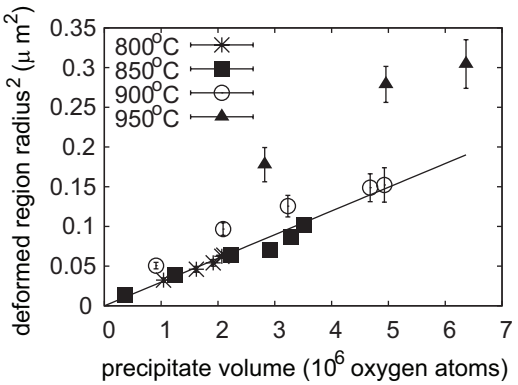

Figure 3 Dependence of size of the deformed region caused by the oxide precipitates in silicon on their volume for various annealing temperatures. The line shows dependence according to formula (4) for $p = 0.08$.

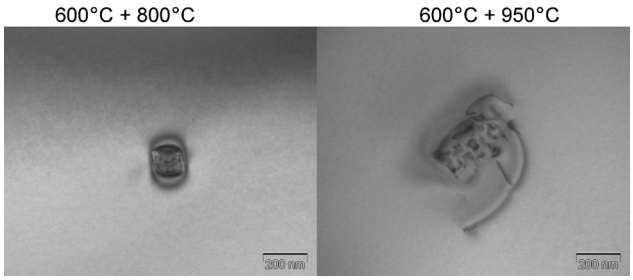

Figure 4 Transmission electron microscopy images on samples annealed at precipitation temperature 800 °C (left) and 950 °C (right) at the end of precipitate growth. The precipitate in the right panel is surrounded by the dislocation loop.

above 850 °C leads to the complexes of the precipitates and dislocation loops. In this case the formulas (1) and (4) are no longer valid due to the dislocation loops contribution. The detailed study of the precipitate–dislocation complexes is a subject of the further work.

4 Dynamical X-ray diffraction in Laue geometry

In order to determine the absolute precipitate concentration we have used the simultaneous measurement of the diffracted and transmitted beam intensity in the Laue diffraction geometry, which gives us more information than the measurement of just the diffraction peak in the Bragg geometry. The intensity was measured as a function of the angle of incidence with respect to the diffracting crystallographic planes and was normalized with respect to the intensity of the primary beam.

The examples of the dynamical diffraction curves measured on the sample with precipitates and without precipitates are shown in Fig. 5. The measurement on the non-annealed sample perfectly corresponds to the classical Laue dynamical diffraction theory of the ideal crystal (see, e.g., Ref. [9]) convoluted with the apparatus function of the Bartels Ge 220 monochromator. This indicates that concentration of other defects in the non-annealed samples is negligible and also the monochromator crystals

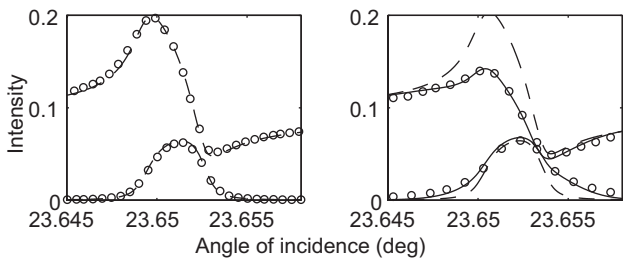

Figure 5 Intensities of transmitted (upper curves) and diffracted (lower curves) beams in Laue 220 diffraction on thin silicon slices without precipitates (left panel) and containing $1.5 \times 10^{11}\,\mathrm{cm}^{-3}$ precipitates (right panel). Circles denote measured data points, dashed lines correspond to dynamical calculation for perfect (defect-free) crystal and solid lines show simulation for crystal containing precipitates. Thicknesses of both samples were 150 μm.

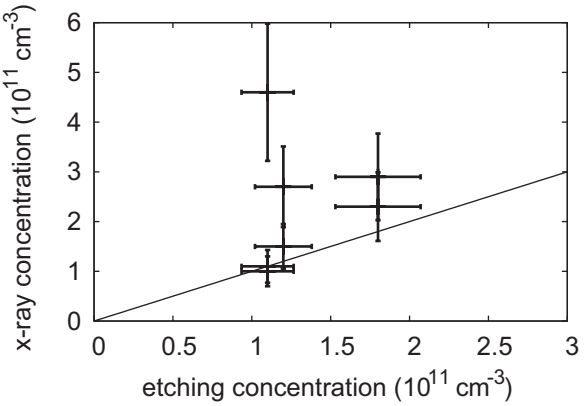

Figure 6 Concentration of the defects determined by the X-ray dynamical diffraction as a function of the concentration determined by the selective etching.

are defect-free. The intensities of the diffracted and transmitted beams at the sample with defects shows strong deviation from the ideal case. In this case, where the sample thickness is a few times larger than the extinction length, the presence of the defects leads to a slight increase of the diffracted intensity and a significant decrease of the transmitted intensity. The width of the diffraction maximum increases.

The diffraction profiles of the samples with precipitates were calculated using theory developed by Holý and Gabrielyan [10]. This theory is based on the solution of Takagi equations in the crystal containing statistically uniform distribution of non-diffracting regions. The input parameters of the calculation are mean defect radius and their concentration. The decrease of the transmitted intensity is roughly proportional to the relative volume of defects in the sample.

In the studied samples the relative volume of defects was up to 5% and the precision of its determination was about $\pm 0.2\%$. The determination of the mean defect radius is less precise especially for small defect concentration, since the defect size affects mostly the width of diffraction curve. The absolute concentration of defects can be calculated from the volume ratio of defects and defect radii, but its value has large uncertainty in the order of about 30%.

The correlation of the precipitate concentration determined using X-ray dynamical diffraction and selective etching is plotted in Fig. 6. We can observe that in the most cases X-ray diffraction gives larger value than the selective etching measurement. However, the precipitate concentration is so high, that the etch pits can overlap and the selective etching could underestimate the precipitate concentration. On the other hand the X-ray diffraction can overestimate their concentration, since it is sensitive to all types of lattice defects. The radii of the defects determined by the dynamical diffraction correspond roughly to the radii of the deformed region determined by the X-ray diffuse scattering described in the previous section. More precise precipitate sizes and subsequently precipitate concentrations could be possibly obtained combining X-ray diffuse scattering and the dynamical diffraction.

5 Conclusion We have shown that the X-ray diffuse scattering does not provide a direct information on the size of the SiO_2 particle embedded in the silicon lattice, however, we can find the size of the strongly deformed region around the precipitate. Moreover combining the X-ray diffraction measurements with other techniques (IR absorption spectroscopy, selective etching, TEM) we can determine the deformation field and namely precipitate volume mismatch p, which is not accessible by other experimental techniques. The measurement of the dynamical diffraction in the Laue geometry can be used to determine the volume fraction of the strongly deformed parts of the crystal and the concentration of the precipitates.

Acknowledgements The authors acknowledge the interest of prof. V. Holý and the help of J. Kuběna during sample preparation. This work was part of the research program MSM0021622410 of the Ministry of education of the Czech republic and was supported by the Czech Science Foundation projects 202/09/1013 and 202/09/P410.

References

[1] B. C. Larson and W. Schmatz, Phys. Status Solidi B **99**, 267 (1980).
[2] L. A. Charnyi, K. D. Sherbachev, and V. T. Bublik, Phys. Status Solidi A **128**, 303 (1991).
[3] P. Klang, V. Holý, J. Kuběna, R. Štoudek, and J. Šik, J. Phys. D: Appl. Phys. **38**, A105 (2005).
[4] ASTM book of standards (1996), chap. F1188, pp. 438–441.
[5] M. A. Krivoglaz, X-ray and Neutron Diffraction in Nonideal Crystals (Naukova Dumka, Kiev, 1983).
[6] V. Holý, U. Pietsch, and T. Baumbach, High-resolution X-ray Scattering from Thin Films and Multilayers (Springer, Oxford, 1998).
[7] O. Caha and M. Meduňa, Phys. B **404**, 4626 (2009).
[8] B. C. Larson, Diffuse Scattering and the Fundamental Properties of Materials (Momentum Press, New Jersey, 2009), pp. 139–160.
[9] A. Authier, Dynamical Theory of X-ray Diffraction (Oxford University Press, Berlin, 2001).
[10] V. Holý and K. T. Gabrielyan, Phys. Status Solidi B **140**, 39 (1987).

